

The following article has been submitted to JASA Express letters. After it is published, it will be found at <http://asa.scitation.org/journal/jel>.

1 **Distributed acoustic sensing recordings of low-**
2 **frequency whale calls and ship noises offshore**
3 **central Oregon**

4 William S. D. Wilcock,^{1,1a} Shima Abadi,^{1,1b} and Brad Lipovsky²

5 ¹ *School of Oceanography, University of Washington, Seattle, WA, 98195* wilcock@uw.edu

6 abadi@uw.edu

7 ² *Department of Earth and Space Sciences, University of Washington, Seattle, WA, 98195*

8 lp17@uw.edu

9

10 Distributed acoustic sensing (DAS) is an optical technique that can measure strain
11 changes along an optical fiber to distances of ~100 km with a spatial sensitivity of
12 tens of meters. In November 2021, 4-days of DAS data was collected offshore on
13 two cables of the Ocean Observatories Initiative Regional Cabled Array that extend
14 offshore central Oregon. Numerous 20 Hz fin whale calls, northeast Pacific blue
15 whale A and B calls, and ship noises were recorded. This data is publicly available to
16 support studies to understand the frequency and spatial sensitivity of submarine
17 DAS for low-frequency acoustic monitoring.

18

19 Keywords: Distributed Acoustic Sensing, Whale Vocalizations, Ship Noise, Fin

20 Whale, Blue Whale, Submarine Cable

^{1a} Author to whom correspondence should be addressed.

^{1b} Also at: School of STEM, Division of Engineering and Mathematics, University of Washington, Bothell

21 1. **Introduction**

22 Low frequency sound within the oceans is generated by a wide number of
23 physical, biological, and anthropogenic sources (Wilcock et al., 2014). These
24 include the wind interacting with the sea-surface, the deformation of sea ice and
25 icebergs, earthquakes, volcanic activity, baleen whale and fish vocalizations, ship
26 propellers and machinery, seismic airguns and pile driving. Passive acoustic
27 monitoring of the ocean soundscape is thus a useful tool to study a variety of
28 processes and to understand the impacts of anthropogenic activities and changing
29 climate on the ocean environment (Duarte et al., 2021). Since sustained hydro-
30 acoustic observations are challenging and expensive to obtain offshore, there is
31 strong motivation to explore new technologies that might enhance our ability to
32 record and characterize sounds within the oceans.

33 Distributed acoustic sensing (DAS) is a relatively new observational
34 technique that interrogates an optical fiber with repeated laser pulses and applies
35 interferometry to the Rayleigh backscattered light to measure changes in strain
36 along the fiber (Hartog, 2017). The method can work to distances of up to ~100
37 km and has a spatial resolution of meters and a broad frequency sensitivity. A
38 DAS fiber optic cable behaves similarly to a long line of closely spaced single-axis
39 broadband seismometers oriented in the direction of the fiber, although DAS
40 measures the spatial derivative of ground velocity (i.e., rate of change of strain)
41 rather than ground velocity (Hartog, 2017).

42

43 The spatial resolution of DAS measurements is termed the gauge length
44 and is controlled by both the duration of the laser pulse and length of time over
45 which each interferometric measurement is averaged. DAS data is commonly
46 collected with a channel spacing that is much smaller than the gauge length.
47 Increasing the gauge length decreases spatial resolution and the sensitivity to short
48 wavelength strain signals but improves the signal to noise of the measurement and
49 thus allows measurements to greater distance from which the backscattered light
50 is more attenuated. The temporal resolution is limited by the two-way travel time
51 of light along the fiber because there should be no more than one light pulse in
52 the fiber at once. For example, for a 100 km long fiber, the maximum laser
53 interrogation rate is ~ 1000 Hz. If the sampling rate is at least a factor of 2 lower
54 than the maximum laser interrogation rate, then successive interrogations can be
55 combined to increase signal to noise.

56 Within industry, DAS has been used for a decade to collect vertical
57 seismic profiles in boreholes (Mateeva et al., 2014). Within academia, DAS is now
58 widely used for a variety of geophysical applications including earthquake studies,
59 seismic imaging and glacier deformation, and it also has application in urban areas
60 for anthropogenic noise sources (Zhan et al., 2019; Lindsey and Martin, 2021).
61 On land, DAS observations can often take advantage of the extensive network of
62 dark fibers that have been laid in urban areas and along transportation corridors
63 to provide growth capacity for telecommunications. In the oceans, DAS
64 experiments are more challenging because submarine telecommunications cables
65 do not generally include dark fibers. Spare fibers in the nearshore portions of
66 cables would be relatively cheap to add but they are of no use for

67 telecommunications without the expensive optical repeaters that are necessary to
68 transmit signals more than ~ 300 km.

69 In 2019, three studies documented the utility of submarine DAS for
70 recording earthquakes and oceanographic signals using data from short tests of on
71 the research infrastructure of the MARS cabled observatory in Monterey Bay
72 (Lindsey et al., 2019), the MEUST deep sea cabled observatory in the
73 Mediterranean off France (Sladen et al., 2019) and a cable in the North Sea off
74 Belgium (Williams et al., 2019). This pioneering work has spurred a rapid growth
75 in interest in submarine DAS including its applications to acoustics.

76 Rivet et al. (2021) showed that DAS could be used to track a tanker
77 passing over the MEUST cable at water depths of both 85 m and 2000 m.
78 Matsumoto et al. (2021) compared DAS and hydrophone recordings of airgun
79 signatures using cable extending offshore Japan to >3000 m water depth. They
80 found both systems were sensitive to airgun signals from 0.1 to tens of Hz
81 although the DAS had lower signal to noise above a few Hz. A comparison of
82 airgun recording between DAS on cable at 100-400 m depth and a towed
83 hydrophone streamer in a shallow Fjord in Norway (Taweessintananon et al., 2021)
84 showed similar noise levels on both systems. Working with the same data set,
85 Bouffaut et al. (2022) present DAS recordings of baleen whales at frequencies up
86 to nearly 100 Hz and demonstrated tracking for animals swimming near the cable.

87 In this paper, we present an overview of a 4-day public-domain submarine
88 DAS experiment that was conducted on two cables extending offshore central
89 Oregon (section 2), demonstrate the capabilities of DAS to recording hydro-
90 acoustic signals (section 3) from fin whale calls (section 3.1), blue whale calls

91 (section 3.2) and ship noises (section 3.3) and discuss the preliminary results and
92 opportunities for future research with these acoustic signals (section 4).

93 **2. OOI DAS Experiment**

94 The Ocean Observatories Initiative Regional Cabled Array (Figure 1,
95 inset) operates two submarine cables that land at Pacific City, Oregon (Smith et
96 al., 2018). The northern cable runs ~500 km west to Axial Seamount while the
97 southern cable extends ~150 km offshore onto the Juan de Fuca plate before
98 wrapping around to the south and east onto the continental slope and shelf off
99 Newport, Oregon. Both cables include a single twisted pair of optical fibers that
100 support 10 Gbps ethernet to primary nodes on the trunk cables that connect via
101 secondary cables and junction boxes to suites of sensors on the seafloor and on
102 moorings.

103 From November 1-5, 2021, a scheduled shutdown of the RCA for
104 maintenance provided an opportunity for a 4-day community fiber sensing
105 experiment to interrogate the fibers in each cable extending out to the first optical
106 repeaters, which are located at 1600 m depth 95 km along the south cable and at
107 600 m depth 65 km along the north cable (Figure 1). These nearshore sections of
108 the cables are buried to a nominal depth of 1.5 m depth below the seafloor. On
109 the south cable DAS data was collected on both fibers using an Optasense
110 QuantX interrogator and a Silixa IDASv3 system. On the north cable DAS data
111 was collected on one fiber with a second Optasense QuantX interrogator while a
112 Silixa ULTIMA SM distributed temperature sensor was deployed on the other
113 fiber. The data has a total volume of 26 TB and can be accessed through a data

114 repository hosted by the University of Washington along with information about
 115 the experiment configuration and data format
 116 ([https://oceanobservatories.org/pi-instrument/rapid-a-community-test-of-](https://oceanobservatories.org/pi-instrument/rapid-a-community-test-of-distributed-acoustic-sensing-on-the-ocean-observatories-initiative-regional-cabled-array/)
 117 [distributed-acoustic-sensing-on-the-ocean-observatories-initiative-regional-cabled-](https://oceanobservatories.org/pi-instrument/rapid-a-community-test-of-distributed-acoustic-sensing-on-the-ocean-observatories-initiative-regional-cabled-array/)
 118 [array/](https://oceanobservatories.org/pi-instrument/rapid-a-community-test-of-distributed-acoustic-sensing-on-the-ocean-observatories-initiative-regional-cabled-array/)).

119 Table 1 summarizes the DAS recording parameters. Although there were
 120 some intervals of recording at sample rates up to 1000 Hz and with gauge lengths
 121 down to 3 m, most of the data were collected with a sample rate of 200 Hz and
 122 gauge length of 30-50 m. These parameters were selected to ensure sufficient
 123 signal to noise to record to near the distal ends of the fibers.

124

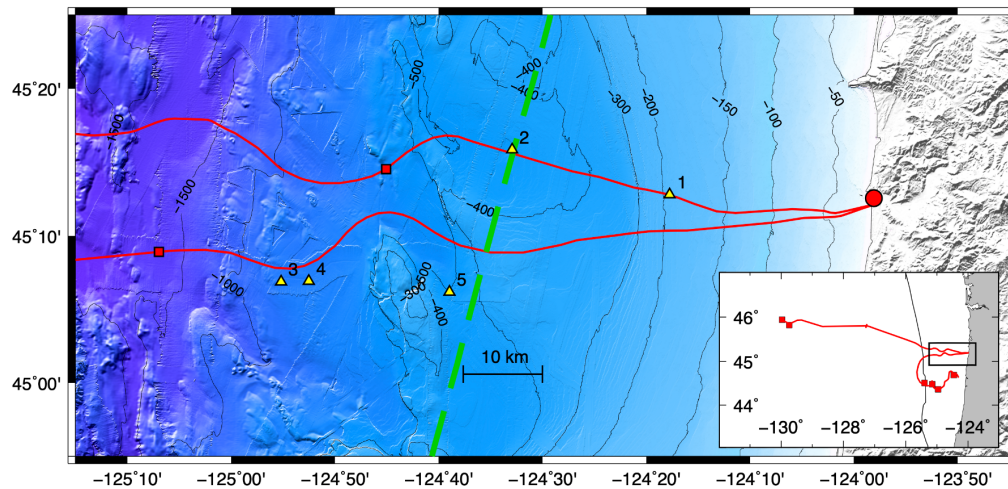
125 TABLE 1. Summary of recording parameters for the OOI RCA DAS
 126 experiment. For each of the 3 DAS interrogators the table identifies the fiber
 127 used, the length of fiber interrogated, the channel spacing, the gauge length and
 128 the sampling frequency with the parameters only listed when they change.

	Optasense - north cable	Optasense - south cable	Silixa - south cable
Nov 1 (2-6 hours)	Testing various configurations	Testing various configurations	Testing on receive fiber of north cable
Nov 1-2	Transmit fiber 65.2 km 2 m channel spacing 30 m gauge length 1000 Hz sampling	Transmit Fiber 95 km 2 m channel spacing 50 m gauge length 200 Hz sampling	Receive Fiber 80.6 km 2 m channel spacing 30 m gauge length 200 Hz sampling
Nov 2-3	500 Hz sampling		

Nov 3-4	50 m gauge length 200 Hz sampling		40.4 km 1 m channel spacing 10 m gauge length
Nov 4-5			19.7 km 3 m gauge length 1000 Hz
Nov 5 (3 hours)	Receive fiber	Receive fiber	Transmit fiber 80.5 km 2 m channel spacing 30 m gauge length 200 Hz

129

130



131

132 Fig. 1. Bathymetric map showing the nearshore portion of the two OOI RCA
 133 cables as red lines, the shore station as a red circle and the first optical repeaters as
 134 red squares. Also shown are the fin whale call locations obtained by time
 135 difference of arrival for the data shown in Fig. 2c, f (numbered yellow triangles)

136 and the northward track of the cargo ship for which data is shown in Fig 4 (bold
137 green dashed line). Contours are labeled in meters and are unevenly spaced (50 m
138 to 200 m depth, 100 m to 500 m depth and 500 m at larger depths). The inset
139 map shows the geometry of the complete RCA cable with primary nodes on the
140 cable as red squares, the area of the main figure as a black box and the base of the
141 continental slope as a faint black line.

142 143 **3. Results**

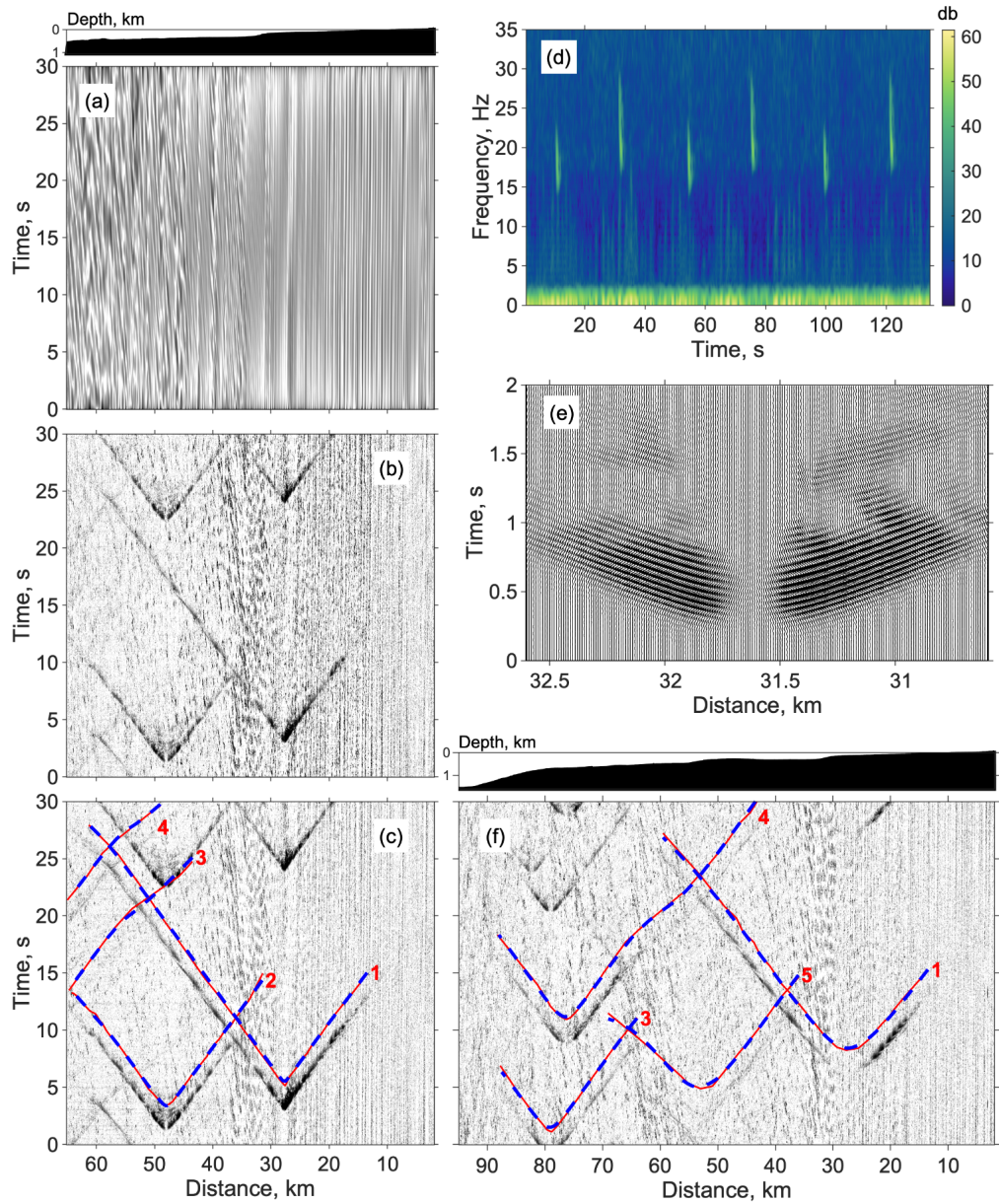
144 The unfiltered DAS data (Fig. 2a) is dominated by the long period signals
145 from ocean surface waves (primary microseisms) in shallow water and secondary
146 microseisms in deeper water (Sladen et al., 2019; Williams et al., 2019) but
147 acoustic signals are readily apparent when the records are filtered above ~ 10 Hz
148 (Fig. 2b). Acoustic signals can be further enhanced by applying an $f-k$ filter to
149 remove signals propagating along the cable at less than the speed of sound (Fig.
150 2c)

151 *2.1. Fin whale vocalizations*

152 The experiment occurred during the breeding season for fin whales and
153 songs of the stereotypical 1-s-long 20-Hz fin whale chirp are recorded
154 throughout. Fin whale calls are observed everywhere along the cables except
155 within about 10 km of the coast. Individual calls are observed out to distances of
156 tens of kilometers, forming a characteristic V-shape in the record sections (Fig 2b-
157 c, f). Spectrograms show that DAS records frequency content of calls with most
158 songs characterized by a doublet pattern of alternating lower and higher frequency

159 notes (Fig. 2d) that now dominates songs in the northeast Pacific (Wierathumeller
160 et al., 2017). The recorded amplitudes are low at the location on the cable closest
161 to the whale (Fig. 2e), as would be expected for a measurement that is sensitive to
162 strain along rather than across the cable.

163 The fin whale calls can be located using time difference of arrival. Figures
164 2c, f show an example where vocalizations from 5 whales can be located at
165 distances that range from 25 km to 75 km offshore and within no more than a
166 few kilometers of one cable (Fig. 1).



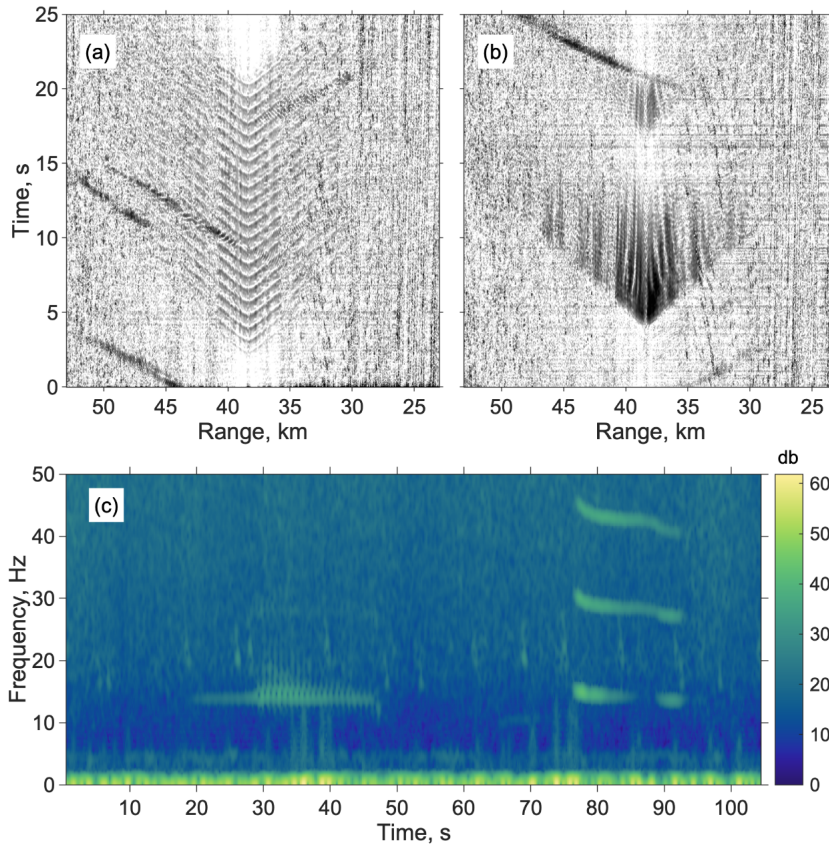
167

168 Fig. 2. Example of fin whale recordings (a) Record section beginning at 04-Nov-
 169 2021 02:00:27 UT, showing 30 s of unfiltered data recorded by the Optasense
 170 interrogator on the north cable. Distance from the interrogator is plotted on the
 171 horizontal axis and time is plotted on the vertical axis with the amplitude envelope
 172 shown by logarithmically scaled shading after normalizing each trace to its median
 173 amplitude. (b) As for (a) except after the application of a 15-27 Hz bandpass
 174 filter. Fin whale arrivals are visible as dark shaded “V” shapes with the apex

175 marking the location on the cable closest to the whale. (c) As for (b) but with a f -
176 k filter to remove all energy with an apparent velocity along the cable less than 1.4
177 km/s. Manual picks of the fin whale arrivals (red solid line) and model times
178 (bold blue dashed line) for a uniform velocity of 1.48 km/s are shown offset 2 s
179 from the fin whale calls and are numbered to indicate the corresponding whale
180 location in Fig. 1. (d) Spectrogram beginning at 02-Nov-2021 18:15:40 UT, for the
181 Silixa interrogator on the south cable, averaged over 100 channels, showing 6
182 notes in a fin whale doublet song. (e) Record section beginning at 02-Nov-2021
183 18:16:54 UT, for the Silixa interrogator showing channels within ~ 1 km of the
184 closest point to a fin whale call. (f) As for (c) but for the Optasense interrogator
185 on the south cable.

186 2.2. *Blue whale vocalizations*

187 The calls of the Northeast Pacific blue whale were much less common
188 during the experiment, but several sequences of the A and B calls are observed
189 (Fig. 3) with the first 3 harmonics of the B call well recorded. In contrast to fin
190 whales, blue whale calls are only recorded out to distances of ~ 10 km.



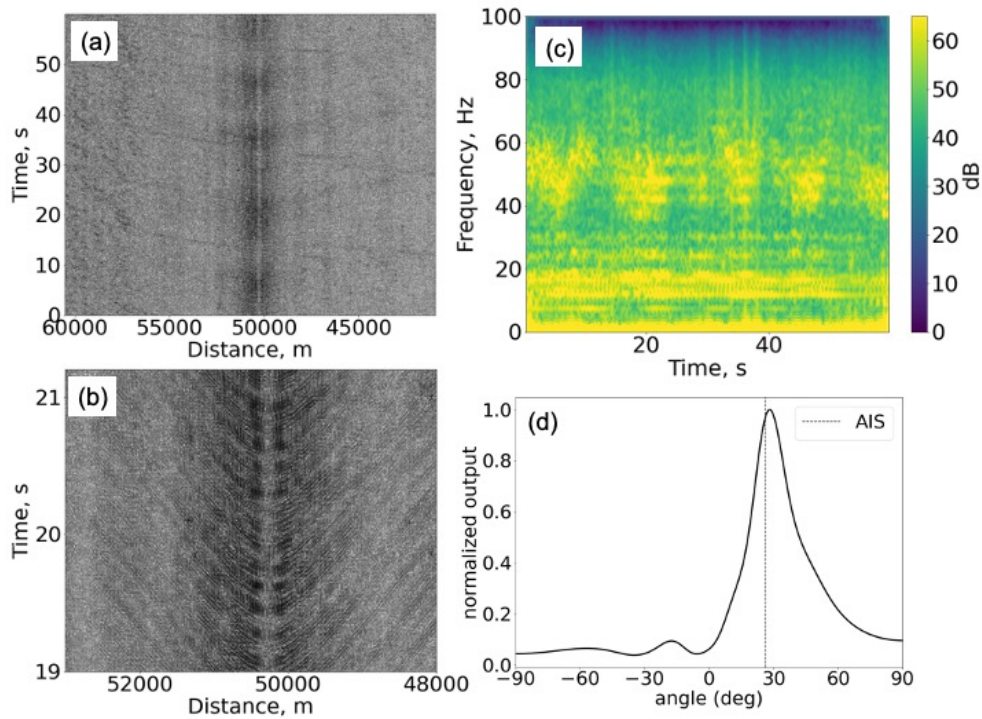
191

192 Fig. 3. Example of Northeast Pacific blue whale recordings on the Silixa
 193 interrogator on the south cable. (a) Record section beginning at 02-Nov-2021
 194 10:36:09 UT, showing an example of an A call with the closest location on the
 195 cable at a distance of 38 km. The A call is overlain by several higher amplitude fin
 196 whale calls. The data have been filtered with a 10.5-18 Hz bandpass filter and an
 197 $f-k$ filter to remove energy propagating along the cable at less than 1.4 km/s. (b)
 198 As for (a) but showing a B call with record section beginning at 02-Nov-2021
 199 10:33:36 UT. Frequency filtering has removed all but the first harmonic. (c)
 200 Spectrogram beginning at 02-Nov-2021 10:32:24 UT, averaged over 100 channels,
 201 showing an A call followed by a B call.

202

203 2.3. Ship Recordings

204 Figure 4 shows an example of ship noise recorded by the Optasense
205 interrogator on both north and south cables. Using the Automatic Identification
206 System (AIS) data, this ship was determined to be a cargo ship of length 180 m
207 that passes above the cable with an approximate speed of 13.2 knots. The data
208 have been filtered with a 10-90 Hz bandpass filter and an $f-k$ filter to remove
209 energy propagating along the cable at less than 1.4 km/s.



210

211 Fig. 4. Example of ship sound recording beginning at 03-Nov-2021 01:57:31 UT,
212 traveling at 13.2 knots over both cables recorded by the Optasense interrogator
213 with a sample rate of 200 Hz and gauge length of 50 m (a) Record section
214 showing 60 s of a cargo ship sound with the closest location on the south cable at
215 a distance of 50 km. (b) Record section showing channels within ~5 km of the

216 closest point to the ship. (c) Spectrogram averaged over 100 channels, showing
217 acoustic energy between 10-60 Hz. (d) Plane-wave beamformer output for the
218 signal shown in (a) using a sub-array of the fiber optic cable consisting of 150
219 channels starting at 49.7 km. The estimated bearing is in agreement with the
220 bearing calculated from the AIS data.

221

222 Compared to fin whale and blue whale calls, ship noises are recorded over
223 a shorter distance (~5 km). The multipath interferences are noticeable in Fig. 4b
224 which could be affected by the ship's motion over the cable, varying coupling of
225 the fiber, different bathymetry along the cable, and fiber curvature. Similar to Fig.
226 2e, the recorded amplitudes are low at the location on the cable closest to the ship
227 (at a distance of 50 km) which is due to the cable sensitivity to strain along rather
228 than across the cable.

229 Plane-wave beamforming (Jensen et al., 1994) is used to calculate the
230 bearing of the vessel relative to a 150-channel sub-array between 49.7-50 km. The
231 beamforming output is maximum at 29.6 degree which is consistent with the
232 bearing of 26 degree calculated using the ship location from the AIS data.

233 **3. Discussion**

234 The OOI community DAS experiment confirms earlier work which
235 shows that buried submarine telecommunication cables can record low frequency
236 acoustic signals. Numerous fin whale calls, blue whale calls, and ship noises were
237 recorded to distances of up to ~40km, 10 km and 5 km, respectively.

238 An important question is why these detection distances differ. Studies
239 suggest that the source levels for fin and blue whales are similar. Average values
240 of 186 (Watkins et al., 1987), 189 (Wierathmueller et al., 2013) and 171 dB re 1
241 μPa at 1 m (Charif et al. 2002) have been reported for fin whales in the northeast
242 Pacific, with the last estimate likely 10-15 dB lower due to the methodology
243 (Wierathmueller et al., 2013). For the B call of the northeast Pacific blue whale,
244 reported values are 180 dB (Thode et al., 2000) and 186 dB re 1 μPa at 1 m
245 (McDonald et al., 2001). While the uncertainties in these estimates are consistent
246 with fin whale calls being somewhat louder, such an explanation for the difference
247 in the maximum detection distance in the DAS data, would be inconsistent with
248 work using ocean bottom seismometers and hydrophones where blue whale B
249 calls are detected to larger ranges (e.g., Wilcock and Hilmo, 2022).

250 The differences may be related to the frequency sensitivity of the DAS
251 data. First, the optical fiber within an armored buried submarine cable may
252 couple better to acoustical strain at lower frequencies. Second, DAS observations
253 average strain changes over the gauge length and when this length approaches or
254 exceeds the signal wavelength, the summed strain change measurements will
255 experience aliasing, reducing the recorded amplitude. The blue whale B call has a
256 significant amount of energy in higher order harmonics and particularly the 3rd
257 harmonic at 40-45 Hz (Thode et al., 2000). The 35 m wavelength of the 3rd
258 harmonic is similar to the 30-50 m gauge length so that at larger distances, when
259 the call is propagating sub parallel to the cable it may be poorly recorded.

260 The reported source levels of commercial ships vary from 177-188 dB re 1
261 μPa at 1 m (McKenna et al., 2012; MacGillivray and de Jong, 2021) which

262 suggests that ships have similar or slightly lower source levels than fin and blue
263 whales. However, ships radiate acoustic energy in a broad frequency range that
264 can go as high as 1000 Hz with most ships having significant energy to ≥ 100 Hz.
265 (McKenna et al., 2012). The ship noises recorded in the OOI DAS experiment
266 do not show acoustic energy above 60 Hz which again would be consistent with
267 reduced sensitivity at higher frequencies as an explanation for the lower detection
268 range.

269 Another potential explanation for differences in detection range could be
270 the depth of the source. Ship propellers are located close to the surface while
271 studies with acoustical tags show that fin and blue whales vocalize at depths of up
272 to a few tens of meters (Oleson et al., 2007; Stimpert et al., 2015; Lewis et al.,
273 2018). With warming ocean surface temperature, the mode excitation depths
274 move deeper than the typical ship source depths and this can cause a reduction in
275 the ship noise band spectral level (Dahl et al, 2021). Additional work is needed to
276 understand the impact of speed of sound profile on the detection range of
277 different sound source recordings on DAS.

278 The DAS sensitivity, as expected, is strongly directional with the recorded
279 amplitudes of both whales (Fig. 2c) and ships (Fig. 4d) very low at the position of
280 closest approach where the propagation direction is perpendicular to the cable.
281 This effect is understood to be due to the cable-longitudinal strain rates being
282 insensitive to plane acoustic waves at normal incidence. It also appears from the
283 fin localizations that whales are only clearly detected on both cables which are
284 spaced ~ 10 km apart, when the curvature of the cables results in the call

285 propagating sub-parallel to both cables (e.g., locations 3 and 4 in Fig. 1 and the
286 corresponding detections in Fig. 2c, f).

287 The OOI DAS experiment recorded tens of thousands of fin whale calls,
288 which provide a remarkable data set both to investigate the directional and depth
289 dependent acoustic sensitivity of DAS near 20 Hz and characterize the spatial
290 distribution, depth of calling and behavior of vocalizing fin whales offshore
291 central Oregon. One of the challenges of DAS is determining accurately the
292 location of each channel, given uncertainties in the path of the fiber and the speed
293 of light in the fiber. A joint inversion for the location of fin whale calls and DAS
294 channels would serve as an analog to the tap tests used to locate fibers on land
295 (Lindsey and Martin, 2021). The fin whale calls can also be exploited to study low
296 frequency sound propagation with water column velocity structure potential
297 including this as an unknown in inversions. Finally, beamforming approaches
298 should be used to explore whether the DAS data can be used to detect fin whales
299 at azimuths and ranges where they are not apparent in the filtered plots.

300 The acoustic signals from ships and whales recorded by the OOI DAS
301 experiment with gauge lengths of 3, 10, 30 and 50 m (Table 1) can be used to
302 understand frequency sensitivity of DAS at lower frequencies and its dependence
303 on gauge length. Such work should motivate future experiments that deploy
304 hydrophones near cables to ground truth recordings and that explore the utility of
305 DAS to detect high-amplitude higher-frequency signals such as those from
306 humpback or sperm whales.

307 DAS generates large data sets; extrapolating the OOI DAS experiment to
308 continuous recordings would generate $O \sim 2$ PB/year of data. To give a sense of
309 scale, six months of data at this rate is about the size of the entire Incorporated
310 Research Institutions for Seismology Data Management Center archive as of April
311 2022 (<https://ds.iris.edu/data/distribution/>). Managing such data volumes will
312 require a variety of approaches. Further work is required to determine optimal
313 channel spacing and to determine whether the 2m channel spacing used in the
314 OOI experiment is justified by its scientific utility. Other approaches could
315 involve a return to the triggered data acquisition paradigm common with seismic
316 data before about the year 2000. A modern approach to triggered acquisition
317 could leverage smart, potentially machine learning-based algorithms run in an
318 edge-computing topology so as to only record signals of interest at high spatial
319 and temporal sampling rates, while still defaulting to a lower rate data that would
320 enable studies of the ambient field. Both lossy and lossless real-time data
321 compression should be considered, and recent results have shown promise in this
322 topic (Dong et al., 2022). The public domain OOI DAS data provides a resource
323 to support the development of such approaches

324 **Acknowledgments**

325 We thank the technical staff of the OOI RCA and field data acquisition
326 team for their work to collect the OOI DAS data set. The data collection was
327 supported by the National Science Foundation under grant OCE-2141047.

328 **References and links**

329 Charif, R. A., Mellinger, D. K., Dunsmore, K. J., Fristrup, K. M., and Clark, C. W.
330 (2002). "Estimated source levels of fin whale (*Balaenoptera physalus*)
331 vocalizations: Adjustments for surface interference," *Mar. Mamm. Sci.*
332 18(1), 81-98.

333 Dahl, P. H., Dall'Osto, D. R., and Harrington, M. J. (2021) "Trends in low-
334 frequency underwater noise off the Oregon coast and impacts of COVID-
335 19 pandemic," *J. Acoust. Soc. Am.* 149, 4073-4077.

336 Dong, B., Popescu, A., Tribaldos, V. R., Byna, S., Ajo-Franklin, J., and Wu, K.
337 (2022). "Real-time and post-hoc compression for data from Distributed
338 Acoustic Sensing," *Comput. Geosci.* 166, 105181.

339 Duarte, C. M., Chapuis, L., Collin, S. P., Costa, D. P., Devassy, R. P., Eguiluz, V.
340 M., ... and Juanes, F. (2021). "The soundscape of the anthropocene
341 ocean," *Science* 371(6529), eaba4658.

342 Hartog, A. H. (2017). "An introduction to distributed optical fibre sensors,"
343 (CRC press. Boca Raton, Florida), 472 pp.

344 Jensen, F., Kuperman, W., Porter, M., and Schmidt, H. (1994). "Computational
345 Ocean Acoustics" (American Institute of Physics, New York), 634 pp.

346 Lewis, L. A., Calambokidis, J., Stimpert, A. K., Fahlbusch, J., Friedlaender, A. S.,
347 McKenna, M. F., ... and Širović, A. (2018). "Context-dependent variability
348 in blue whale acoustic behaviour," *Royal Soc. open Sci.* 5(8), 180241.

349 Lindsey, N. J., and Martin, E. R. (2021). "Fiber-optic seismology," *Ann. Rev.*
350 *Earth Planet. Sci.* 49, 309-336.

351 Lindsey, N. J., Dawe, T. C., and Ajo-Franklin, J. B. (2019). “Illuminating seafloor
352 faults and ocean dynamics with dark fiber distributed acoustic sensing,”
353 Science 366(6469), 1103-1107.

354 McDonald, M. A., Calambokidis, J., Teranishi, A. M., and Hildebrand, J. A.
355 (2001). “The acoustic calls of blue whales off California with gender
356 data,” J. Acoust. Soc. Am. 109(4), 1728-1735.

357 MacGillivray, A. and de Jong, C. (2021). “A reference spectrum model for
358 estimating source levels of marine shipping based on automated
359 identification system data,” J. Mar. Sci. Eng. 9(4), 369.

360 Mateeva, A., Lopez, J., Potters, H., Mestayer, J., Cox, B., Kiyashchenko, D., ...
361 and Detomo, R. (2014). “Distributed acoustic sensing for reservoir
362 monitoring with vertical seismic profiling,” Geophys. Prospect. 62(4),
363 679-692.

364 Matsumoto, H., Araki, E., Kimura, T., Fujie, G., Shiraishi, K., Tonegawa, T., ...
365 and Karrenbach, M. (2021). “Detection of hydroacoustic signals on a
366 fiber-optic submarine cable,” Sci. Rep. 11(1), 1-12.

367 McKenna, M. F., Ross, D., Wiggins, S. M., Hildebrand, J. A. (2012). “Underwater
368 radiated noise from modern commercial ships,” J. Acoust. Soc. Am.
369 131(1), 92-103.

370 Oleson, E. M., Calambokidis, J., Burgess, W. C., McDonald, M. A., LeDuc, C.
371 A., and Hildebrand, J. A. (2007). “Behavioral context of call production by
372 eastern North Pacific blue whales”, Mar. Ecol. Prog. 330, 269-284.

373 Rivet, D., de Cacqueray, B., Sladen, A., Roques, A., and Calbris, G. (2021).
374 “Preliminary assessment of ship detection and trajectory evaluation using

375 distributed acoustic sensing on an optical fiber telecom cable,” *J. Acoust.*
376 *Soc. Am.* 149(4), 2615-2627.

377 Sladen, A., Rivet, D., Ampuero, J. P., De Barros, L., Hello, Y., Calbris, G., and
378 Lamare, P. (2019). “Distributed sensing of earthquakes and ocean-solid
379 Earth interactions on seafloor telecom cables,” *Nat. Commun.* 10(1), 1-8.

380 Smith, L. M., Barth, J. A., Kelley, D. S., Plueddemann, A., Rodero, I., Ulses, G.
381 A., ... and Weller, R. (2018). “The ocean observatories initiative,”
382 *Oceanogr.* 31(1), 16-35.

383 Stimpert, A. K., DeRuiter, S. L., Falcone, E. A., Joseph, J., Douglas, A. B.,
384 Moretti, D. J., ... and Goldbogen, J. A. (2015). “Sound production and
385 associated behavior of tagged fin whales (*Balaenoptera physalus*) in the
386 Southern California Bight,” *Anim. Biotelemetry* 3(1), 1-12.

387 Taweesintananon, K., Landrø, M., Brenne, J. K., and Haukanes, A. (2021).
388 “Distributed acoustic sensing for near-surface imaging using submarine
389 telecommunication cable: A case study in the Trondheimsfjord, Norway,”
390 *Geophys.* 86(5), B303-B320.

391 Thode, A. M., D’Spain, G. L., and Kuperman, W. A. (2000). “Matched-field
392 processing, geoacoustic inversion, and source signature recovery of blue
393 whale vocalizations,” *J. Acoust. Soc. Am.* 107(3), 1286-1300.

394 Watkins, W. A., Tyack, P., Moore, K. E., and Bird, J. E. (1987). “The 20-Hz
395 signals of finback whales (*Balaenoptera physalus*),” *J. Acoust. Soc. Am.*
396 82(6), 1901-1912.

397 Weirathmueller, M. J., Wilcock, W. S. D., and Soule, D. C. (2013). “Source levels
398 of fin whale 20 Hz pulses measured in the Northeast Pacific Ocean,” J.
399 Acoust. Soc. Am. 133(2), 741-749.

400 Weirathmueller, M. J., Stafford, K. M., Wilcock, W. S., Hilmo, R. S., Dziak, R. P.,
401 and Tréhu, A. M. (2017). “Spatial and temporal trends in fin whale
402 vocalizations recorded in the NE Pacific Ocean between 2003-2013,”
403 PLoS One 12(10), e0186127.

404 Wilcock, W. S. D., Stafford, K. M., Andrew, R. K., and Odom, R. I. (2014).
405 “Sounds in the ocean at 1–100 Hz,” Ann. Rev. Mar. Sci. 6(1), 117-140.

406 Wilcock, W. S. D., and Hilmo, R. S. (2021). “A method for tracking blue whales
407 (*Balaenoptera musculus*) with a widely spaced network of ocean bottom
408 seismometers,” PLoS One 16(12), e0260273.

409 Williams, E. F., Fernández-Ruiz, M. R., Magalhaes, R., Vanthillo, R., Zhan, Z.,
410 González-Herráez, M., and Martins, H. F. (2019). “Distributed sensing of
411 microseisms and teleseisms with submarine dark fibers,” Nat. Commun.
412 10(1), 1-11.

413 Zhan, Z. (2019). “Distributed Acoustic Sensing Turns Fiber- Optic Cables into
414 Sensitive Seismic Antennas,” Seismol. Res. Lett. 91, 1–15.